Targeting IL-6 trans-signalling by sgp130Fc attenuates severity in SARS-CoV-2 -infected mice and reduces endotheliopathy

María Ángeles Rodríguez-Hernández,[a,*] Mercedes Baena-Bustos,[b] David Carneros,[a] Carola Zurita-Palomo,[a] Pablo Muñoz-Pinillos,[c] Jaime Millán,[c] Francisco Javier Padillo,[a] Cristian Smerdou,[d] Cayetano von Kobbe,[c] Stefan Rose-John,[e] and Matilde Bustos[a,**]

[a]Area of Liver, Digestive and Inflammatory Diseases, Institute of Biomedicine of Seville (IBiS), Virgen del Rocio University Hospital (HUVR), Spanish National Research Council (CSIC), University of Seville (US), Seville, Spain
[b]Pneumology Unit, Institute of Biomedicine of Seville (IBiS), Virgen Macarena University Hospital (HUVM), Spanish National Research Council (CSIC), University of Seville (US), Seville, Spain
[c]Centro de Biología Molecular Severo Ochoa (CBM), CSIC-UAM, Cantoblanco, Madrid, Spain
[d]Division of DNA and RNA Medicine, Cima Universidad de Navarra, Instituto de Investigación Sanitaria de Navarra (IdISNA), and CCUN, Pamplona, Spain
[e]Institute of Biochemistry, Kiel University, Kiel, Germany

eBioMedicine
2024;103: 105132
Published Online xxx
https://doi.org/10.1016/j.ebiom.2024.105132

Summary

Background SARS-CoV-2 infection is considered as a relapsing inflammatory process with a dysregulation of IL-6 signalling. Classic IL-6 signalling is thought to represent a defence mechanism against pathogens. In contrast, IL-6 trans-signalling has pro-inflammatory effects. In severe COVID-19, therapeutic strategies have focused on global inhibition of IL-6, with controversial results. We hypothesized that specific blockade of IL-6 trans-signalling could inhibit inflammatory response preserving the host defence activity inherent to IL-6 classic signalling.

Methods To test the role of the specific IL-6 trans-signalling inhibition by sgp130Fc in short- and long-term consequences of COVID-19, we used the established K18-hACE2 transgenic mouse model. Histological as well as immunohistochemical analysis, and pro-inflammatory marker profiling were performed. To investigate IL-6 trans-signalling in human cells we used primary lung microvascular endothelial cells and fibroblasts in the presence/absence of sgp130Fc.

Findings We report that targeting IL-6 trans-signalling by sgp130Fc attenuated SARS-CoV-2-related clinical symptoms and mortality. In surviving mice, the treatment caused a significant decrease in lung damage. *In vitro*, IL-6 trans-signalling induced strong and persisting JAK1/STAT3 activation in endothelial cells and lung fibroblasts with proinflammatory effects, which were attenuated by sgp130Fc. Our data also suggest that in those cells with scant amounts of IL-6R, the induction of gp130 and IL-6 by IL-6:sIL-6R complex sustains IL-6 trans-signalling.

Interpretation IL-6 trans-signalling fosters progression of COVID-19, and suggests that specific blockade of this signalling mode could offer a promising alternative to mitigate both short- and long-term consequences without affecting the beneficial effects of IL-6 classic signalling. These results have implications for the development of new therapies of lung injury and endotheliopathy in COVID-19.

Funding The project was supported by ISCIII, Spain (COV-20/00792 to MB, PI23/01351 to MARH) and the European Commission—Next generation EU (European Union) (Regulation EU 2020/2094), through CSIC's Global Health Platform (PTI Salud Global, SGL2103029 to MB). PID2019-110587RB-I00 (MB) supported by MICIN/AEI/10.13039/501100011033/and PID2022-143034OB-I00 (MB) by MICIN/AEI/10.13039/501100011033/FEDER. MAR-H acknowledges support from ISCIII, Spain and the European Commission—Next generation EU (European Union), through CSIC's Global Health PTI.

*Corresponding author.
**Corresponding author.
E-mail addresses: marodriguez-ibis@us.es (M.Á. Rodríguez-Hernández), mbustos-ibis@us.es (M. Bustos).

Keywords: IL-6 trans-signalling; sgp130Fc; SARS-CoV-2; K18-hACE2 transgenic mice; COVID-19; Endotheliopathy

Research in context

Evidence before this study

New strategies specifically blocking different modes of IL-6 signalling by small molecules and antibodies represent promising alternatives for the management of inflammatory diseases. IL-6 trans-signalling is recognized as the predominant pathway by which IL-6 promotes disease pathogenesis and development. The importance of IL-6 trans-signalling in SARS-CoV-2 infection has been suggested but must be thoroughly investigated. Selective targeting of IL-6 trans-signalling could offer advantages, such as reduced infections, over global IL-6 blockade in COVID-19.

Added value of this study

The study provides evidence of the beneficial effect of IL-6 trans-signalling inhibition in short- and long-term consequences of SARS-CoV-2 infection *in vivo*. In mice, the specific IL-6 trans-signalling inhibitor, sgp130Fc, reduced mortality and symptomatology caused by the infection. Furthermore, the treatment attenuated lung injury in surviving mice. *In vitro*, we demonstrated that sgp130Fc inhibited IL-6 trans-signalling effects on primary human lung microvascular endothelial cells and lung fibroblasts. Our data also suggest that gp130 induction could sustain IL-6 trans-signalling in cells with scant amounts of IL-6R.

Implications of all the available evidence

Our results demonstrating the implication of IL-6 trans-signalling in COVID-19 could help to understand the pathogenesis and progression of the disease. Our findings support the use of therapies focused on the specific blockade of IL-6 trans-signalling to mitigate both, acute phase and long-term consequences of COVID-19.

Introduction

SARS-CoV-2 triggered the dreadful global pandemic coronavirus disease 2019 (COVID-19) at the end of 2019. Although widespread vaccination has made clinically less deadly,[1] there is currently no established an effective therapy for it. Additional research is still imperative in order to find a reliable treatment and to mitigate short and long-term consequences.

One of the main characteristics of SARS-CoV-2 infection is the intense inflammation,[2] together with thrombotic incidents and coagulopathy,[3] particularly in those who have severe sickness. Lung pathologies include diffuse lung alveolar damage with neutrophils and macrophages that cause alveolar-capillary barrier dysfunction.[4] It has been reported that endotheliopathy observed in COVID-19 results from both direct mechanisms of virus infection,[5] and indirect mechanisms such as massive release of cytokines,[6] among others interleukin (IL)-6, IL1-β and tumour necrosis factor (TNF-α).[7] Research efforts have partially allowed the understanding of the pathophysiology of SARS-CoV-2 infection; however, key questions regarding factors implicated in the fatal outcomes of the disease remain incompletely known.

IL-6 is a key cytokine of inflammatory states. IL-6 signal transduction starts by the binding to membrane-bound form of the IL-6 receptor (IL-6R) or its soluble form (sIL-6R), generated by proteolytic shedding in tissues expressing membrane IL-6R or by alternative splicing. In both events, those complexes of IL-6 bind to the membrane signal transducer glycoprotein 130 (gp130), expressed in all cells. In the classical signalling, the activity provoked by IL-6 and membrane IL-6R results in a homeostatic, protective, anti-inflammatory effect, representing a defence mechanism against pathogens. In contrast, activity of IL-6 with sIL-6R has pro-inflammatory effects and is known as trans-signalling.[8] Emerging evidence reveals that IL-6 trans-signalling plays a key role in inflammation, endothelial cell activation, coagulopathy and thrombosis observed in fatal COVID-19.[9,10] In this context, we have previously reported the importance of analysing IL-6 signalling components in serum to identify patients at risk of fatal COVID-19. High levels of IL-6, sIL-6R, soluble (s)gp130 and [IL-6:sIL-6R]/[IL-6:sIL-6R:sgp130] complex ratio were independent predictors of severity and mortality. We demonstrated that a combined analysis of IL-6 signalling components offers an accurate and robust model to predict severity.[11] The study was in line with the concept that interactions between IL-6 and its receptors have a direct impact on the different modes of signalling. Thus, the evaluation of those components is crucial to ensure an appropriate and valid interpretation of serum IL-6 levels. Remarkably, only studies with a global blockade of both IL-6 classic and trans-signalling with IL-6R neutralizing monoclonal antibodies as sarilumab and tocilizumab have been reported in COVID-19, showing beneficial effects on survival rates.[12–15] Nevertheless, this global blockade of IL-6 may predispose patients to an increased risk of infections.[16,17] The specific inhibition of IL-6 trans-signalling could constitute an alternative option with beneficial effects. Hence, we hypothesized that therapies targeting IL-6 trans-signalling in patients with COVID-19, could block inflammation preserving the physiologic and host defence activities inherent to classic IL-6 signalling. Indeed, there are preclinical studies of neoplastic and human autoimmune diseases wherein the specific blockade of IL-6 trans-signalling has clear advantages

over global blockade of IL-6. To note, sgp130Fc only bounds IL-6 in the presence of sIL-6R, therefore inhibiting IL-6 trans-signalling while conserving classic signalling. This specific inhibitor has demonstrated therapeutic potential in different preclinical models.[18] New sgp130Fc variants have emerged as a great promise for therapy such as olamkicept for inflammatory bowel disease, in clinical trials.[19,20] Experimental molecules such as the designer protein c19s130Fc, which blocks SARS-CoV-2 viral infection and IL-6 trans-signalling, have been proven *in vitro*.[21]

The K18-hACE2 transgenic mouse infected with SARS-CoV-2 is recognized as a valuable model for investigating the pathological mechanisms of COVID-19. Indeed, this model closely displays the COVID-19 phenotypes observed in the intensive care unit,[22] with lung inflammation, multiorgan failure and dead, and it is widely used to assess novel therapeutic approaches.[23–27] Here, using this established model, we demonstrate that targeting IL-6 trans-signalling by sgp130Fc attenuates SARS-CoV-2-related clinical symptoms and mortality. Moreover, in surviving mice the treatment reduces lung damage. Importantly, our *in vitro* studies show that IL-6 trans-signalling induces strong and persisting Janus kinase1/signal transducer and activator of transcription3 (JAK1/STAT3) activation on endothelial cells and lung fibroblasts with proinflammatory effects, partially attenuated by sgp130Fc. Overall, this study reveals that IL-6 trans-signalling is implicated in the pathogenesis and progression of COVID-19, and suggests that specific blockade of this signalling mode could offer a promising alternative to mitigate both, acute phase and long-term consequences of this disease. These results have implications in the clinical management of COVID-19 and in the development of new therapies.

Methods

Animal experiments

K18-hACE2 humanized mice (SN34860-B6.Cg-Tg (K18-ACE2)2Prlmn/J) were obtained from The Jackson Laboratory. This mouse strain has been previously used as a model for SARS-CoV-2-induced disease and it presents biochemical and lung pathological changes compatible with human severe disease.[23–27] Eight-month-old male K18-hACE2 transgenic mice were inoculated intranasally with 25 μL of Modified Eagle Medium (MEM) containing 1×10^4 plaque forming units (PFU) of SARS-CoV-2. To note, only male animals were used due to the existing evidence supporting the notion that SARS-CoV-2 infected male mice display higher mortality than female, which reflects the epidemiological data regarding COVID-19.[28,29] Sample size of 17 animals/group were determined using Library Trial Size for sample size calculation in clinical research (R package), using the function: TwoSampleproportion.Equality. We accepted an alpha risk of 0.05 and a beta risk of 0.10 and anticipated mortality of 60% and 25% in untreated and treated groups, respectively. Mice were randomly distributed in two groups: SARS-CoV-2-infected (n = 17) and SARS-CoV-2-infected and sgp130Fc-treated mice (n = 18). Moreover, a control group (mock, non-infected, n = 4). sgp130Fc was used at the dose of 1 mg/kg, as it has been previously reported and only inhibits trans-signalling,[30] and administered by intraperitoneal injection (i.p.) twice: at two and eight days after virus inoculation. Mock and untreated infected animals received phosphate buffered saline (PBS) as vehicle i.p. Mouse weight and health were monitored daily, up to 15 days post infection (dpi) (end of experiment) or until they reached end-point criteria (body weight loss >20% or >13%–16% together with other symptoms related to breathing rate (dyspnoea), appearance (hunched posture, piloerection and eye closure), and behaviour (lethargy/staggering and non-response to stimuli). Data were obtained from two independent experiments. All experiments with SARS-CoV-2 were performed in a Biosafety level 3 (BSL3) Laboratory at the Veterinary Health Surveillance Center (VISAVET, Complutense University of Madrid), after two weeks of acclimatisation period.

Ethics

Animal experiments with virus infection were carried out conformed to the Guide for the Care and Use of Laboratory Animals published by the National Academy of Sciences in accordance with the Spanish legislation (BOE 34/2013), EU Directive 2010/63/EU. The protocol was approved by the animal ethics committee of Comunidad de Madrid (PROEX 087.0/21).

Virus and sgp130Fc

SARS-CoV-2 virus (isolate Navarra-2473) was obtained from nasopharyngeal swab of a patient with COVID-19 hospitalized in the University of Navarra Clinic (Pamplona, Spain) in April 2020, after obtaining written informed consent and acquiring the necessary Regional Government permits, as it has been previously reported.[27,31] Initially, the virus sample was used to infect Vero-E6 cells (ATCC® CRL-1586™, RRID:CVCL_0574) which were grown with MEM containing 10% foetal bovine serum (FBS) and antibiotics. Cell supernatants were collected at 48 h post-inoculation and titrated using a lysis plate assay in Vero-E6 cell monolayers, resulting in a titter of 4.3×10^7 PFU/mL. The viral stock was quickly frozen in a methanol-dry ice bath and stored at –80 °C. For subsequent experiments, smaller aliquots of the original stock were prepared, obtaining a titter of 1.8×10^7 PFU/mL after being frozen again.

sgp-130Fc was kindly provided by Dr. S. Rose-John. This fusion protein was generated by linking the entire extracellular portion of human gp130 to the Fc portion of human IgG1. The protein bound IL-6 only in the

presence of sIL-6R and consequently specifically inhibits IL-6 trans-signalling without affecting classic signalling.[32]

Lung extraction

The right lung was inflated with formalin (4%) and fixed with the same buffer for seven days before being embedded in paraffin for histological analysis. The left lung lobe was used for RNA extraction (cellular and viral), as described below.

Reverse transcriptase-quantitative polymerase chain reaction (RT-qPCR) analysis

For RNA extraction, lung tissue samples were incubated with RNAlater, and subsequently frozen at −80 °C or processed directly according to the RNeasy Plus Micro kit (Qiagen, Hilden, Germany) protocol. For extraction of viral RNA by nasal swabs, samples were collected at four dpi and processed using a MagMax core kit (Applied Biosystems, Woburn, MA, USA) according to the manufacturer instructions. qPCR in lungs and swabs to specifically detect SARS-CoV-2 RNA was performed according to the indications of the COVID-19 dtec-RT-qPCR test kit (F100 format, Genetic PCR Solutions, Orihuela, Spain). For detection of cytokines/chemokines mRNA expression, cDNA was obtained by PrimeScript RT from Takara Clontech (Takara Biomedical Technology, Beijing, China). qPCR was performed using LightCycler 96 system thermocycler and SYBR Green (Roche, Basel, Switzerland). Product quantities were calculated by applying the ΔCt method ΔCt = (Ct of gene of interest—Ct of housekeeping genes). The housekeeping genes used for input normalization were cyclophilin or RPLO. Primers for qPCR are listed in Supplementary Table S1.

Cytokines and chemokines levels in serum and supernatants from cultured cells

Serum levels of IL-6, sIL-6R, C-X-C motif chemokine ligand 10 (CXCL10, also known as Interferon-γ-induced protein 10, IP-10), C-C motif ligand 5 (CCL5, Rantes), CCL11 (Eotaxin), TNF-α, IFN–γ, IL-1α, IL-10 and sgp130 were analysed using two pre-configured multiplex panels (Mouse Cytokine/Chemokine Magnetic Bead Panel Cat. # MCYTOMAG-70K, –70K-PMX, –70K-PX32, 70PMX25BK and 70PMX32BK; Mouse Soluble Cytokine Receptor Magnetic Bead Panel Cat. # MSCRMAG-42K) from Sigma–Aldrich (St Louis, MO, USA). The experiment was performed in a Bio-Plex 200 System (Bio-Rad Laboratories, Inc., Hercules, CA, USA). Enzyme-linked immunosorbent assay (ELISA) in supernatants from human cultured cells were performed according to the manufacturer's instructions: sgp130 (DuoSet DY228), CCL2/MCP-1 (DuoSet DY279-05), ICAM-1/CD54 (DuoSet DY720-05), from R&D Systems (Minneapolis, MN, USA); IL-6 from ImmunoTools (Friesoythe, Germany, Ref. 31670069).

Histological processing

Lung fixed tissue sections (3 μm) from mice of each experimental group were obtained to perform Haematoxylin-Eosin (H&E), Masson's Trichrome staining, immunohistochemistry and immunofluorescence. P (Tyr705)-STAT3 (Ref. 9131) was purchased from Cell Signalling (Danvers, MA, USA). P-Selectin (CD62P) (Ref. ab255822) and vascular cell adhesion molecule-1 (VCAM1) (Ref. ab134047) antibodies were from Abcam (Cambridge, UK). von Willebrand factor (vWF) antibody (Ref. BS-100448R) was from Thermo Fisher Scientific and isolectin B4 biotin conjugate (Ref. L2140) from Sigma–Aldrich. PolyStain 2-Step Plus Kit, HRP for 3,3′-diaminobenzidine tetrahydrochloride DAB, Rabbit (NB-23-00050-3, NeoBiotec, Nanterre, France) was used to enhance antibody signal. Nuclei were stained using Mayer's haematoxylin. Secondary antibodies labelled with Alexa Fluor™ 555 (Ref. A21428), Alexa Fluor™ 488 (Ref. A11008), Streptavidin-Alexa Fluor™ 555 (S21381) were from Thermofisher Scientific and mounting medium with DAPI (ab104139 from abcam) was applied to cover slides before imaging. Images were captured using Olympus Bx-61 (Olympus, Tokyo, Japan) and Thunder Dmi8 (Leica, Wetzlar, Germany) microscopes.

Imaging analysis

Quantification of number and area of dense inflammation foci, lymphocyte accumulation and % of P-STAT-3 positive cells were performed using ImageJ/FIJI software.[27] Expression of P-Selectin was quantified according to the method recently reported by Granai M et al.[33] Briefly, 5–7 histological sections were analysed for each mouse of the different experimental groups, and five hot-spot regions per section were chosen using an area of 416,000 μm^2 with QuPath software. Areas with artefacts, such as tissue-tear, folding or background noise were excluded. Quantification of P-Selectin positive cells were performed independently in large and small vessels. The values were obtained as percentage of positive cells. Expression of vWF and VCAM1 was quantified as it has been reported by McConnell et al.[34] Briefly, 5–7 histological sections were analysed for each mouse of the different experimental groups. vWF and VCAM1 positive areas in each histological section were quantified in four randomly selected regions in an unbiased fashion using ImageJ/FIJI software. The values were obtained as percentage of positive area.

Human primary cell cultures

Human primary lung microvascular endothelial cells (HMVEC-L-Lung MV Endo, EGM-2MV, CC-2527, Lonza, Basel, Switzerland) were cultured using CC-3202 EGM-2 MV BulletKit (CC-3156_CC-4147, Lonza). Human primary umbilical vein endothelial cells (HUVEC) (CC-2517, Lonza) were cultured using H3CC-3124 medium (EGM TM BulletKit TM (CC-3124), Lonza). Human primary lung IMR-90 fibroblasts (ATCC®

CCL186™, ATCC, Manassas, VA, USA) were cultured using MEM supplemented with 10% FBS. Cells were cultured in 5% CO_2 at 37 °C. Recombinant human proteins were purchased from R&D Systems: IL-6 (Ref. 206-IL-05/CF); IL-6Rα (Ref. 227-SR-025); sgp130Fc Chimera (Ref. 671-GP-100). Cells, at passage 3–6, were cultured in serum-free medium overnight and then stimulated by IL-6 (20 ng/mL), sIL-6R (20 ng/mL), and IL-6:sIL-6R (20 ng/mL) complex in the presence or absence of sgp130Fc (300 ng/mL) for 15 min, 24 h or 48 h.

Western blots

Cell lysates were obtained using lysis buffer (150 mM NaCl, 1 mM EDTA, 25 mM Tris (pH 7.5), 1 mM orthovanadate, 1% triton, and protease inhibitor cocktail (Roche)). Protein concentration was determined by DC protein assay (Bio-Rad). Proteins were separated 7.5 %–12% SDS-PAGE in the presence of a reducing agent (2-mercaptoethanol) and were transferred to polyvinylidene difluoride (PVDF) membranes (Bio-Rad) and stained with Ponceau red solution (Sigma–Aldrich). Primary antibodies against P (Tyr705)-STAT3 (Ref. 9131), STAT3 (Ref. 30,835), P (Tr1034/1035)-JAK1 (Ref. 74,129), JAK1 (Ref. 3344) were purchased from Cell Signalling (Danvers, MA, USA); gp130 (Ref. sc-656) from Santa Cruz Bt. (Santa Cruz, CA, USA); GADPH (Ref. 1461) from StemCell Tech (Vancouver, Canada). Anti-rabbit and Anti-mouse horseradish peroxidase-conjugated secondary antibodies were from Sigma–Aldrich (Ref. 12–348 and Ref. 12–349, respectively). The proteins were detected with enhanced chemiluminescence (Ref. 1705061, Bio-Rad) in a ChemiDoc Imaging System (Bio-Rad) and the densitometric analysis was performed using the software Image Lab 6.0 (BioRad).

Endothelial barrier function assays

Transendothelial electric resistance (TEER) assays with an electric cell-substrate impedance sensing system (1600R; Applied Biophysics) were performed as described,[35] using multifrequency mode ranging between 250 and 64,000 Hz.

Statistics

Analyses were performed with GraphPad Prism 8.4.2, IBM SPSS Statistics 22 software and R studio i386 4.1.2. Sample normality was screened using Shapiro–Wilk test and graphical method quantile–quantile (Q–Q) plot. Levene's test was used to verify homogeneity of variance. When this assumption was not met (p value < 0.05), Welch test was conducted to compare means. Comparisons between the values for different variables were analysed by one-way Analysis of Variance (ANOVA) with Student's t test (for normal variables), Kruskal Wallis test with Mann–Whitney U-test (for non-normal variables) and Chi-square test of Independence (for qualitative variables). Fisher's Exact test in 2 × 2 contingency tables was considered when the expected observations were less than 5 in at least 20% of the tiles. When tables were of order greater than 2 × 2, likelihood ratio was also observed. Overall, a p value < 0.05 was considered statistically significant. Univariate binary logistic regression analysis was used to model the odds that the event *exitus* took place including the single predictor variable *getting treatment*. p value was calculated as a function of Wald chi-squared. Cumulative incidence was performed by Kaplan–Meier analysis, and statistical significance was determined by log-rank test. For survival analysis, origin and start time were the day of virus inoculation (0 dpi) and time of the follow-up was 15 days (15 dpi). During this timeframe, time-to-event for mice that died or had to be sacrificed attending to animal suffering criteria was considered the day of death. On the other hand, animals that survived for the entire duration of the study were sacrificed at 15 dpi. The median (IQR) of the follow-up time was 10 days (7–15) for non-treated group, and 15 days (7.5–15) for treated group. COX proportional hazards regression was used to estimate both the hazard of dying and developing symptoms. Proportional hazards assumption held has been validated using cox.zhp function of R Library (Survival).

Role of funding sources

The funding body did not play any role in study design, data collection, analyses, interpretation, or writing of report.

Results

IL-6 trans-signalling inhibition by sgp130Fc reduces severity and mortality in an experimental model of COVID-19

To investigate IL-6 trans-signalling inhibition by sgp130Fc in COVID-19, we used K18-hACE2 transgenic mice intranasally infected with a sub-lethal dose of SARS-CoV-2 (10^4 PFU); this dose has been previously validated by us.[27] Infected animals were divided into two groups: i) untreated mice injected i.p. with vehicle and ii) treated mice, receiving sgp130Fc (1 mg/kg) i.p. twice, at two and eight days post infection (dpi). K18-hACE2 uninfected mice served as controls (mock). Mice were monitored daily until 15 dpi, the scheduled endpoint of the experiment, by the same researchers in a blinded manner (Fig. 1a). Infected mice that presented endpoint criteria (body weight loss >20% or > 13%–16% plus other symptoms such as dyspnoea, hunched posture, lethargy/staggering, and piloerection) were euthanized. The viral load, at four dpi, were similar in all infected mice regardless of treatment (Fig. 1b). Importantly, the survival rate was significantly superior in sgp130Fc-treated mice compared to untreated animals (Fig. 1c). In infected group, the proportion of

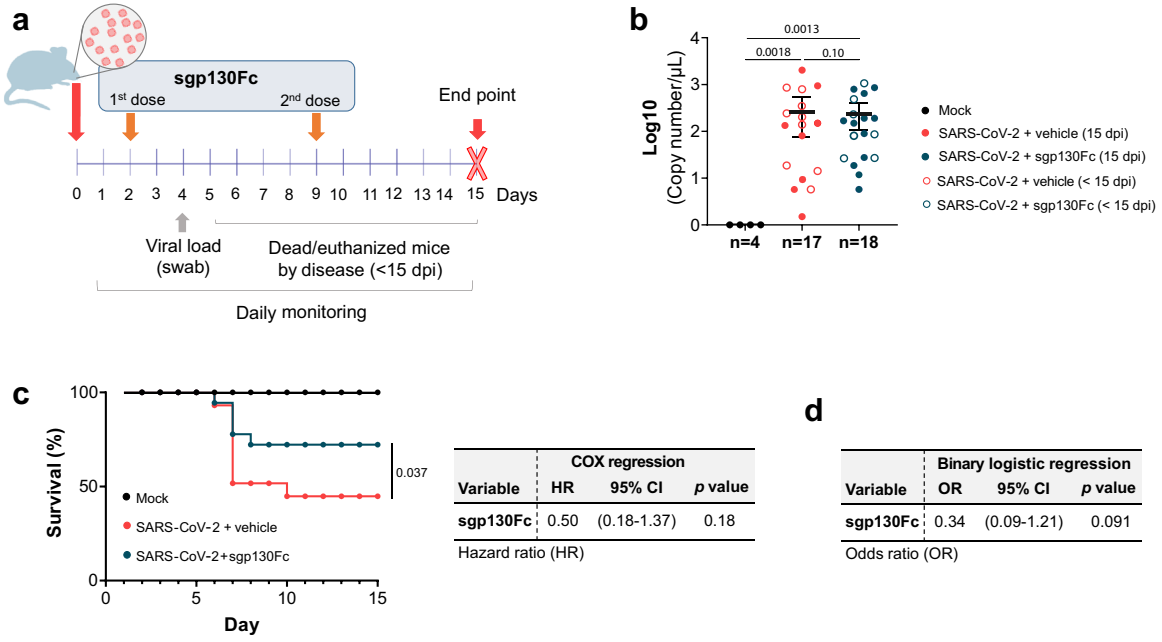

Variable	COX regression HR	95% CI	*p* value
sgp130Fc	0.50	(0.18-1.37)	0.18

Hazard ratio (HR)

Variable	Binary logistic regression OR	95% CI	*p* value
sgp130Fc	0.34	(0.09-1.21)	0.091

Odds ratio (OR)

Fig. 1: **Experimental scheme and impact of IL-6 trans-signalling inhibition by sgp130Fc in SARS-CoV-2 infection-related mortality in K18-hACE2 mice. a)** Experimental design for the animal study. Eight-month-old male K18-hACE2 mice were divided into three groups: i) mock (n = 4); ii) SARS-CoV-2 infected mice injected i.p. with vehicle (PBS) (n = 17); iii) SARS-CoV-2 infected and treated i.p. with sgp130Fc at 1 mg/kg per dose (n = 18). Mice were daily monitored until 15 dpi (experimental end-point). **b)** Viral load obtained from nasal swabs at four dpi quantified by qPCR. Sample size (n) of each group is indicated. Graph shows mean and 95% confidence intervals (CI) with each dot representing an individual animal. Statistics were calculated by Kruskal–Wallis test with Mann–Whitney U-test. **c)** Percentage of mice survival. COX regression analysis for sgp130Fc. HR: Hazard ratio. **d)** Univariate binary logistic regression analysis. *p* values were calculated as a function of Wald chi-squared. OR: odds ratio. Data are combined from two independent experiments. <15 dpi: dead/euthanized mice before the end of the experiment. 15 dpi: surviving mice at the end of experiment.

untreated mice that died or were euthanized before the scheduled endpoint of the experiment (<15 dpi) was significantly higher (55.17%) than those that received sgp130Fc treatment (29.41%). Treatment reduced the risk of dying during the follow-up by 50% (based on a hazard ratio (HR) of 0.5) (Fig. 1c). Moreover, univariate binary logistic regression test revealed that treated mice were 33.85% less likely to die than non-treated animals, highlighting the protective role of the treatment (Fig. 1d).

All SARS-CoV-2 infected mice displayed similar body weight change starting at five dpi (Supplementary Figure S1). However, the evaluation of other clinical symptoms such as irregular breathing (dyspnoea), appearance (hunched posture, piloerection and eye closure) and spontaneous and provoked behaviour (lethargy and non-response to stimuli) (Supplementary Table S2), revealed a significant reduction in the number of animals presenting at least one of these symptoms in the treated group compared to untreated from eight dpi onwards (Fig. 2a). sgp130Fc treatment reduced the percentage of animals that exhibited the mentioned sickness parameters at any time during the follow-up period. Although some of those differences were not statistically significant between the groups, the global analysis suggests the clinical relevance of the treatment (Fig. 2b). The cumulative symptomatology incidence was significant lower in the treated group and COX regression analyses revealed that sgp130Fc treatment had a protective role against development of symptoms (HR 0.62) (Fig. 2c). Since lungs are one of the main SARS-CoV-2 target organs, presence of viral RNA was analysed post-mortem. Viral load was significantly increased in infected mice, with similar values in all groups (treated/untreated and survivors/dead-euthanized animals), while non-infected resulted in absence of viral RNA (Fig. 2d). Overall, our findings indicate that IL-6 trans-signalling blockade by sgp130Fc reduces SARS-CoV-2 infection associated mortality as well as severity of the symptoms in surviving mice (15 dpi).

sgp130Fc decreases proinflammatory cytokines/chemokines in SARS-CoV-2- infected mice

Lung inflammation is one of the main causes of fatal COVID-19.[36] To identify the inflammatory mediators

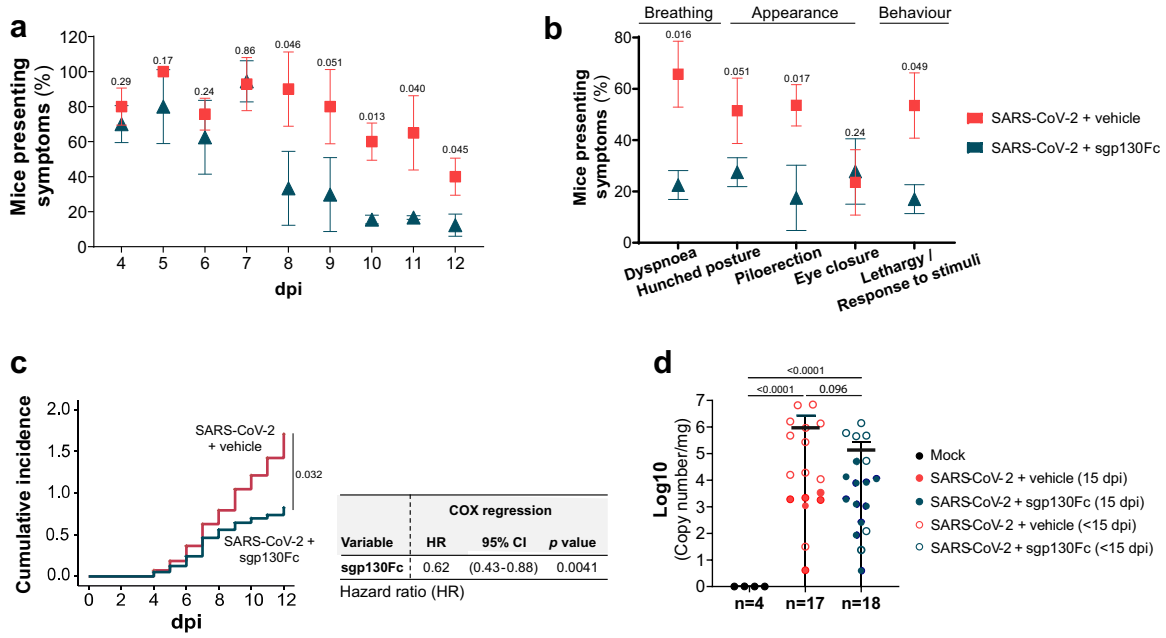

Fig. 2: **Effect of targeting IL-6 trans-signalling by sgp130Fc in symptomatology in SARS-CoV-2 infected mice.** Analysed symptoms consisted on dyspnoea, hunched posture, piloerection and lethargy/staggering. **a)** Percentage of mice presenting at least one of the symptoms previously described. Daily significant differences between experimental groups were determined by Chi-squared test. **b)** Percentage of mice presenting individual symptoms considered as positive when a mouse showed it at any day during the period of follow-up. Significant differences between experimental groups were determined by Chi-squared test. **c)** Cumulative incidence of symptomatology during the follow-up timeframe and COX regression hazard model for sgp130Fc in the context of symptomatology development. HR: Hazard ratio. **d)** Viral load in lung tissue post-mortem (<15 dpi and 15 dpi) quantified by RT-qPCR. Graph shows mean and 95% confidence intervals (CI). Mock (n = 4); SARS-CoV-2 + vehicle (n = 17); SARS-CoV-2 + sgp130Fc (n = 18). Data are combined from two independent experiments. Statistics were calculated by Kruskal–Wallis test with Mann–Whitney U-test. dpi: days post infection. <15 dpi: dead/euthanized mice before the end of the experiment. 15 dpi: surviving mice at the end of experiment.

involved in the pathogenesis of SARS-CoV-2 as well as the potential impact of the specific blockade of IL-6 trans-signalling, we measured the levels of cytokines and chemokines in serum and lung homogenates. Infected dead/euthanized mice (<15 dpi) showed higher systemic levels of IL-6, CXCL10 (IP10), CCL5 (Rantes), CCL11 (Eotaxin), TNF-α, IFN–γ, and sgp130 than surviving mice (15 dpi), regardless of treatment (Fig. 3 and Supplementary Figure S2). In contrast, in the untreated group, levels of sIL-6R were significantly reduced in dead compared to surviving mice (Fig. 3a), as it has been reported in patients who died from COVID-19.[11] Nevertheless, surviving sgp130Fc-treated mice had lower levels of both, IL-6 and sIL-6R, than alive untreated mice (Fig. 3a). These observations are in concordance with previous results obtained from patients with moderate COVID-19, in whom increased levels of both proteins were indicators of severity.[11,37] Levels of sgp130 in survivors were similar between treated and untreated mice (Fig. 3a). Importantly, CCL11 was increased in dead/euthanized mice, as it has been reported in severe COVID-19.[38] Although its function remains unknown, it is elevated during neuroinflammatory response[39]; thus, we can speculate that this chemokine has a role in the neuroinflammatory processes of the infected mice. To determine the impact of the treatment in SARS-CoV-2 infected mice, we determined mRNA expression of cytokines and chemokines associated to disease progression in lung homogenates. As expected, higher levels of pro-inflammatory genes were detected in non-survivors (<15 dpi). Notably, when we focused on infected surviving mice (15 dpi), those that received sgp130Fc showed significant decreased mRNA expression of pro-inflammatory cytokines (*Tnfα*, *Il1ß* and *Ifnγ*), as well as IL-6 family of cytokines and receptors related with severe COVID-19: *Il6r*, *Il6st*, *Osm*, *Osmr*, *Lif*, *Lifr*,[40,41] (Fig. 3b). Collectively, our data suggest that sgp130Fc treatment reduces the expression of inflammatory markers associated to disease progression, in line with milder symptoms developed by these mice.

Targeting IL-6 trans-signalling by sgp130Fc ameliorates lung damage in SARS-CoV-2-infected mice

We next examined the effect of IL-6 trans-signalling inhibition in lungs from SARS-CoV-2 infected mice by histological analyses. Macroscopic inspection of the lungs

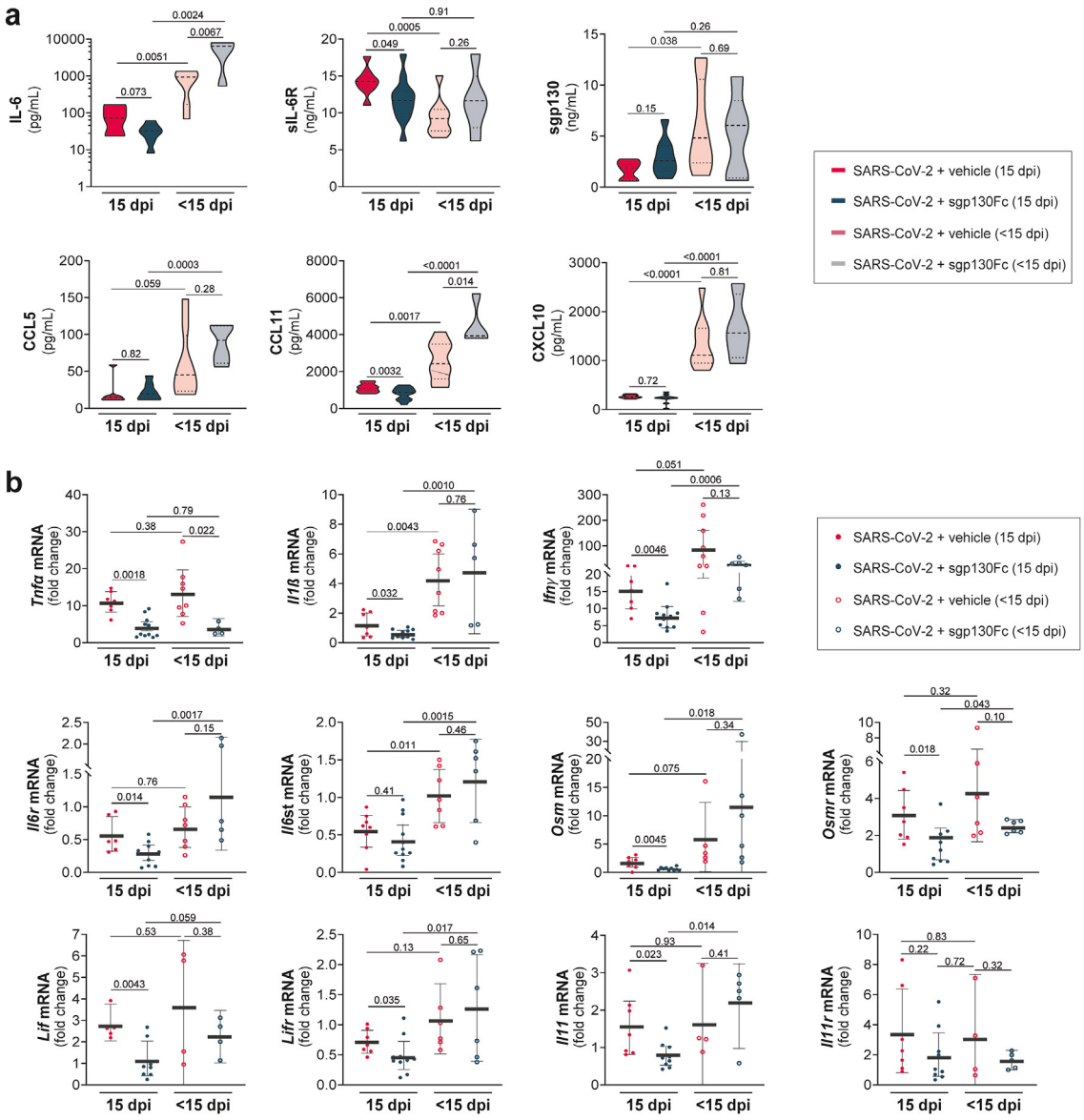

Fig. 3: **Impact of IL-6 inhibition by sgp130Fc in cytokines/chemokines levels in serum and lung tissues from SARS-CoV-2 infected mice.** **a)** Serum levels of the indicated proteins quantified by multiplex platform in each experimental group. **b)** mRNA expression of the indicated cytokines and chemokines in lung tissue measured by qPCR. Control is set to 1 for each experiment and data is presented as fold-change *vs* control (mean and 95% CI). SARS-CoV-2 + vehicle 15 dpi (n = 8); SARS-CoV-2 + sgp130Fc 15 dpi (n = 12). SARS-CoV-2 + vehicle <15 dpi (n = 9); SARS-CoV-2 + sgp130Fc < 15 dpi (n = 6). Data are combined from two independent experiments. Statistics were calculated by Kruskal–Wallis test with Mann–Whitney U-test. *p* values are indicated in the graphs. dpi: days post infection. < 15 dpi: dead/euthanized mice before the end of the experiment. 15 dpi: surviving mice at the end of experiment.

from dead/euthanized mice (<15 dpi) showed that all infected mice displayed alterations, including haemorrhagic, oedematous, or congestive areas, without differences between treated and untreated animals. Histologic examination of the lungs from mice of each experimental group was carried out to determine whether specific inhibition of IL-6 trans-signalling affected disease severity. SARS-CoV-2 infected dead/euthanized mice (<15 dpi), both treated and untreated, showed similar histopathological findings, characterized by multifocal lesions with a tendency to confluence, alveolar oedema and intense haemorrhage indicating breakdown of the vascular integrity as it has been previously reported.[42] A significant interstitial leukocyte infiltration with the presence of neutrophils and mononuclear inflammation was observed in swelling interalveolar spaces, inside the

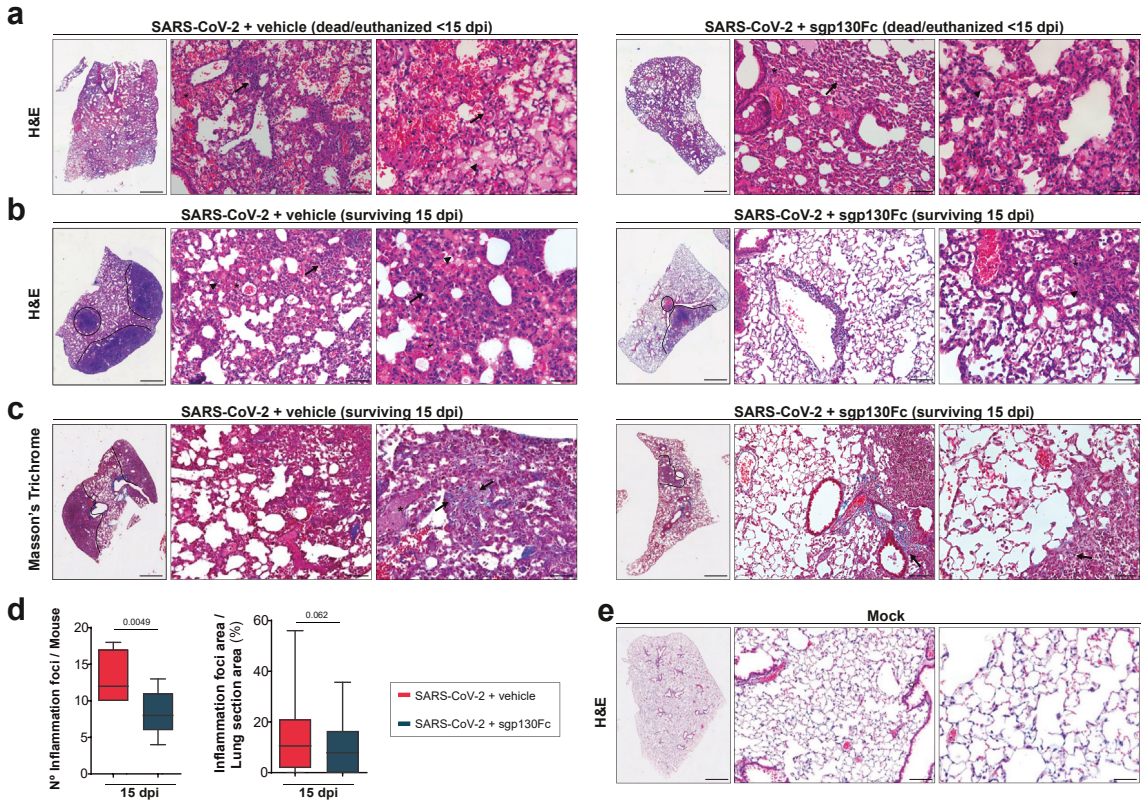

Fig. 4: **Histopathological analysis of lungs from sgp130Fc-treated SARS-CoV-2 infected mice.** Representative images of lung sections from mice of each experimental group. **a)** H&E stain from dead/euthanized SARS-CoV-2-infected animals (<15 dpi), untreated (vehicle) and sgp130Fc treated. Pictures show multifocal lesions, alveolar haemorrhage (asterisk), oedema (black arrowhead), inflammatory infiltrates (black arrow) (50 X, 200 X and 400 X). **b)** H&E stain from surviving SARS-CoV-2-infected animals (15 dpi), untreated and sgp130Fc-treated. Inflammatory foci (dash lines) (50 X) and cells, mainly lymphocytes (black arrow) (200 X and 400 X) are indicated. **c)** Masson's trichrome stain from surviving SARS-CoV-2-infected animals (15 dpi), untreated and sgp130Fc-treated (50 X). Deposits of connective tissue interposed between lymphocytes (black arrow) (200 X and 400 X). **d)** Number of inflammatory foci per mouse and % of inflammatory foci area per lung section area quantified by ImageJ/FIJI software in surviving mice (15 dpi). Graphs show mean and 95% CI. Statistics were calculated by Student's t-test. *p* values are indicated in the graphs. **e)** H&E stain from uninfected animals (mock; 50 X, 200 X and 400 X). Scale bars: 50 X (3000 µm), 200 X (100 µm) and 400 X (50 µm). SARS-CoV-2 + vehicle 15 dpi (n = 8); SARS-CoV-2 + sgp130Fc 15 dpi (n = 12). SARS-CoV-2 + vehicle <15 dpi (n = 9); SARS-CoV-2 + sgp130Fc < 15 dpi (n = 6). Data are combined from two independent experiments. H&E: Haematoxylin Eosin. dpi: days post infection. < 15 dpi: dead/euthanized mice before the end of the experiment. 15 dpi: surviving mice at the end of experiment.

alveoli and surrounding vessels (Fig. 4a). By contrast, the histopathological findings in infected survivors (15 dpi) showed differences between untreated and sgp130Fc-treated mice. The former group presented moderate to severe inflammatory infiltrates mainly composed of lymphocytes and some histiocytes along with neutrophils and macrophages inside of alveoli. Surviving sgp130Fc-treated mice (15 dpi) displayed a more moderate interstitial pattern with a reduction of lung cell infiltration, as well as less deposits of connective tissue intermingled with lymphocytes, in comparison to untreated mice (Fig. 4b and c). We quantified areas of inflammation, considering individual foci and areas with merged of numerous individual foci. In surviving mice (15 dpi), sgp130Fc treatment resulted in a significant decrease of both number of inflammatory foci per animal (37% of reduction) as well as areas of lung inflammation (30% of reduction) compared to untreated group (Fig. 4d). As expected, lungs from non-infected mice did not show histological alterations (Fig. 4e).

To determine the effectiveness of sgp130Fc treatment, we assessed *Stat3* and target genes mRNA: *Lrg1* (*leucine rich alpha-2-glycoprotein 1*), *Saa1* (*serum amyloid a 1*) and *Socs3* (*suppressor of cytokine signalling 3*) in lung samples from SARS-CoV-2 infected mice. A significant overexpression of those genes in dead/euthanized mice (<15 dpi) was observed, regardless treatment. Focussing on survivors (15 dpi), STAT3 dependent genes were significantly downregulated in lungs from sgp130Fc-treated *vs* non-treated mice (Fig. 5a). To identify target interaction in the injured lung we evaluated the expression of P (Tyr705)-STAT3 (P-STAT3) by

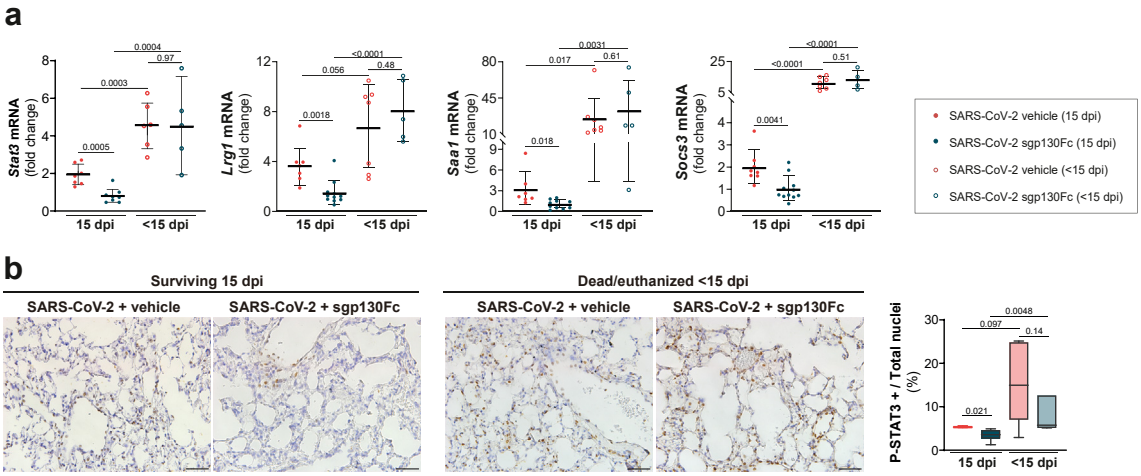

Fig. 5: **STAT3 target genes expression in lung tissue from sgp130Fc-treated SARS-CoV-2 infected mice. a)** mRNA expression of *Stat3, Lrg1, Saa1* and *Socs3* in lungs quantified by qPCR. Control is set to 1 for each experiment and data presented as fold-change *vs* control. **b)** Immunohistochemistry of P (Tyr705)-STAT3 in lung samples. Scale bars: 200 X (100 µm). Data are presented as % of positive cells. SARS-CoV-2 + vehicle 15 dpi (n = 8); SARS-CoV-2 + sgp130Fc 15 dpi (n = 12). SARS-CoV-2 + vehicle <15 dpi (n = 9); SARS-CoV-2 + sgp130Fc < 15 dpi (n = 6). Data are combined from two independent experiments. All graphs show mean and 95% CI. Statistics were calculated by Kruskal–Wallis test with Mann–Whitney U-test (a), and ANOVA with Student's t-test (b). *p* values are indicated in the graphs. dpi: days post infection. < 15 dpi: dead/euthanized mice before the end of the experiment. 15 dpi: surviving mice at the end of experiment.

immunohistochemistry and quantified positive cells. Fig. 5b shows significant decrease of P-STAT3 positive cells in survivors sgp130Fc-treated *vs* untreated. All dead/euthanized mice showed higher number of P-STAT3 positive cells. Moreover, STAT3 is a major regulator of Th17 responses. The expression profiles of factors related to Th17 cells (RAR-related orphan receptors (RORγt), IL-17) and Treg cells (Forkhead box P3 (FoxP3) and IL-10) in lung tissues showed that survivors presented a lower ratio of RORγt/FoxP3 mRNA expression *vs* death/euthanized animals. In surviving group, sgp130Fc-treated mice exhibited the lowest RORγt/FoxP3 ratio (Supplementary Figure S3). Altogether, our results indicate that STAT3 pathway plays a key role in the actions of sgp130Fc, being responsible for the outcomes. Furthermore, an altered Tregs and Th17 cells ratio could be one of the mechanisms responsible for the loss ability to control inflammation in fatal SARS-CoV-2 infected mice, also described in severe COVID-19.[43] Although in most of the sgp130Fc-treated mice the dose was sufficient to inhibit IL-6 trans-signalling, we observed variability that could affect to the homogeneity of our results. It can be speculated that sublethal dose of the virus could infect different organs and replicates with high variability in K18-hACE2 mice, as it has been reported.[44,45] Also, blockade is never complete and small remaining amounts of active IL-6:sIL-6R complexes could probably be sufficient to trigger pro-inflammatory cytokines, especially in a highly inflammatory environment like lungs in SARS-CoV-2 infected mice. Finally, other factors such as cytokines/chemokines could substitute the effects of IL-6:sIL-6R complexes, independently producing pro-inflammatory responses.

Inflammatory processes play an important role in the activation of endothelial cells (directly or by immune-mediated manner),[46,47] being key players in lung inflammation, oedema, and disseminated coagulation with a clear impact in the development of COVID-19.[5,47,48] Immunohistochemical analysis of adhesion molecules in lungs, showed upregulation of CD62P (P-Selectin), a marker of endothelial cells and platelets activation, in all SARS-CoV-2 infected mice. P-Selectin was expressed in endothelial cells and platelet aggregates adhered to endothelium, as it has been reported in the early phase of COVID-19 (vascular phase).[33] Dead/euthanized groups (treated and untreated) showed quite close P-Selectin immunostaining. Surprisingly, a marked staining was observed in surviving mice (15 dpi) on the luminal surface of vessels, endothelial cells and platelet aggregates, with significant increased levels in untreated in comparison to sgp130Fc-treated mice in large and microcirculatory vessels (Fig. 6a). Other endothelial cell activation markers described in COVID-19, including vWF and VCAM1,[49,50] were analysed. vWF expression was found in endothelium as well as in oedematous fluid and thrombi. VCAM1 immunostaining was detected in endothelial cells mainly from large vessels. As we observed in P-Selectin, dead/euthanized mice did not show differences in the expression of those endothelial cell activation markers regardless treatment. Consistently, in survivors, sgp130Fc-treated mice showed significant decreased expression of vWF (% positive area) compared to untreated (Fig. 6b), although VCAM1 immunostaining

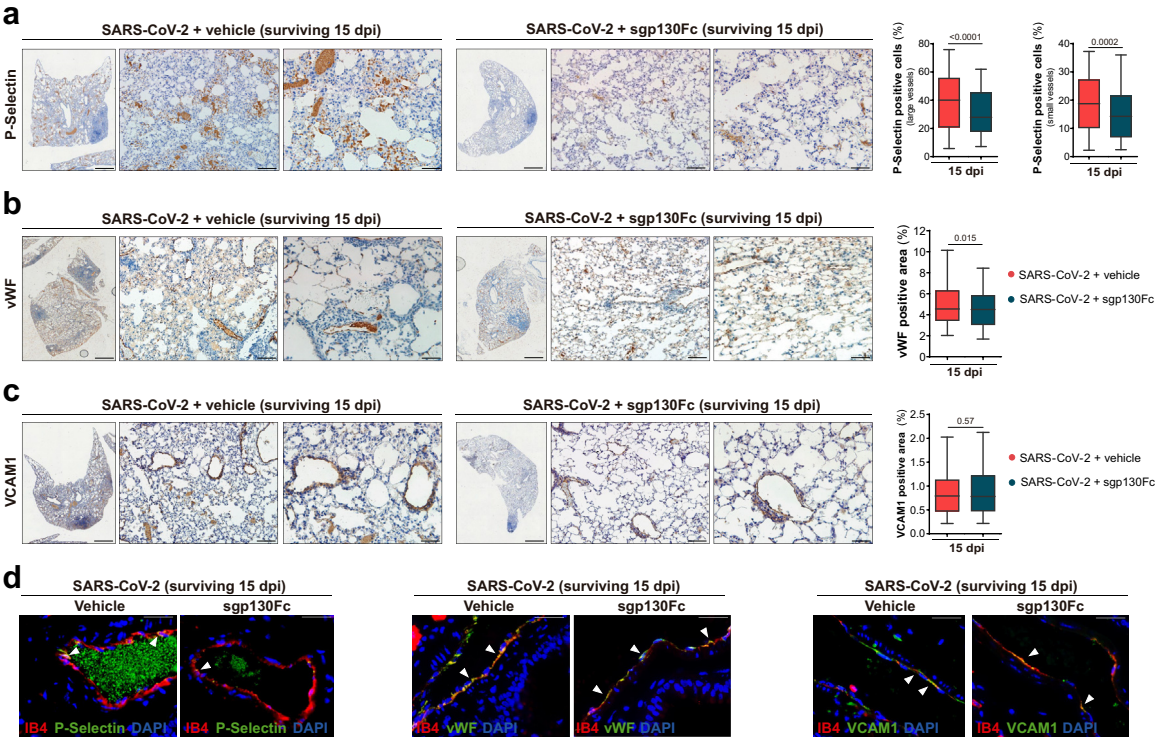

Fig. 6: **Impact of IL-6 trans-signalling inhibition by sgp130Fc on endothelial cells activation in lungs from SARS-CoV-2 infected surviving mice (15 dpi).** Representative immunostaining images of lung sections from surviving groups (15 dpi). **a)** Immunoreaction of P-Selectin on luminal surface of endothelial cells and platelet aggregates (50 X, 200 X and 400 X). Positive cells were quantified using QuPath software. Data are presented as % of positive cells (mean ± SEM). **b)** vWF immunostaining in mural thrombus, oedematous fluid in alveoli and endothelial cells. Positive area was quantified using ImageJ/FIJI software. Data are presented as mean ± SEM. **c)** Immunoreaction of VCAM1 on vascular endothelial cells (50 X, 200 X and 400 X). Positive area was quantified using ImageJ/FIJI software. **d)** Co-localization of endothelial cells (labelled with isolectin B4) with P-Selectin/vWF/VCAM1 in lung tissues by immunofluorescence (400 X). Scale bars: 50 X (3000 µm), 200 X (100 µm) and 400 X (50 µm). SARS-CoV-2 + vehicle 15 dpi (n = 8); SARS-CoV-2 + sgp130Fc 15 dpi (n = 12). 15 dpi: surviving mice at the end of experiment. All graphs show mean and 95% CI. Statistics were calculated by Student's t-test. *p* values are indicated in the graphs.

showed similar values in these groups (Fig. 6c). P-Selectin, mainly expressed in platelet aggregates, vWF and VCAM1 co-localized in lung endothelial cells (Fig. 6d). Collectively, these findings indicate that lung damage was more intense in infected mice that died or had to be euthanized in the first 7–8 days after infection, without differences between treated and untreated mice. Importantly, in survivors, sgp130Fc treatment reduced lung injury, with a significant decrease of inflammatory infiltrate and markers of endothelial cell activation. In summary, targeting IL-6 trans-signalling mitigated lung injury in the SARS-CoV-2-infected mice and it could represent a potential therapy with impact in long term consequences of COVID-19.

sgp130Fc inhibits the effects of IL-6 trans-signalling on human primary endothelial cells and fibroblasts

In severe COVID-19, the release of massive inflammatory cytokines during the cytokine storm leads to endothelial activation, alveolar-capillary barrier dysfunction and fibrosis.[51] We assessed the role of IL-6 trans-signalling in human lung microvascular endothelial cells (HLMVEC), human umbilical vein endothelial cells (HUVEC) and human lung fibroblast (IMR-90). Cells were treated with IL-6 alone or with the IL-6:sIL-6R complex (trans-signalling) as described in methods for 15 min, 24 h and 48 h. We found that JAK1/STAT3 activation by IL-6:sIL-6R complex was strong and persisting (24 h and even 48 h) (Fig. 7a, Supplementary Figure S4). Although the expression of IL-6R in human endothelial cells is not well understood, our results indicate that HLMVEC and IMR-90 represent cell types that primarily express functional IL-6R, as it has been reported in liver sinusoidal endothelial cells,[34] in clear contrast with HUVEC. Our findings provide insights into the dual response of HLMVEC to IL-6: vascular protection *vs* inflammation. To note, sgp130Fc was used to further analyse the role of IL-6 trans-signalling, resulting in a partial blockade of phosphorylation of

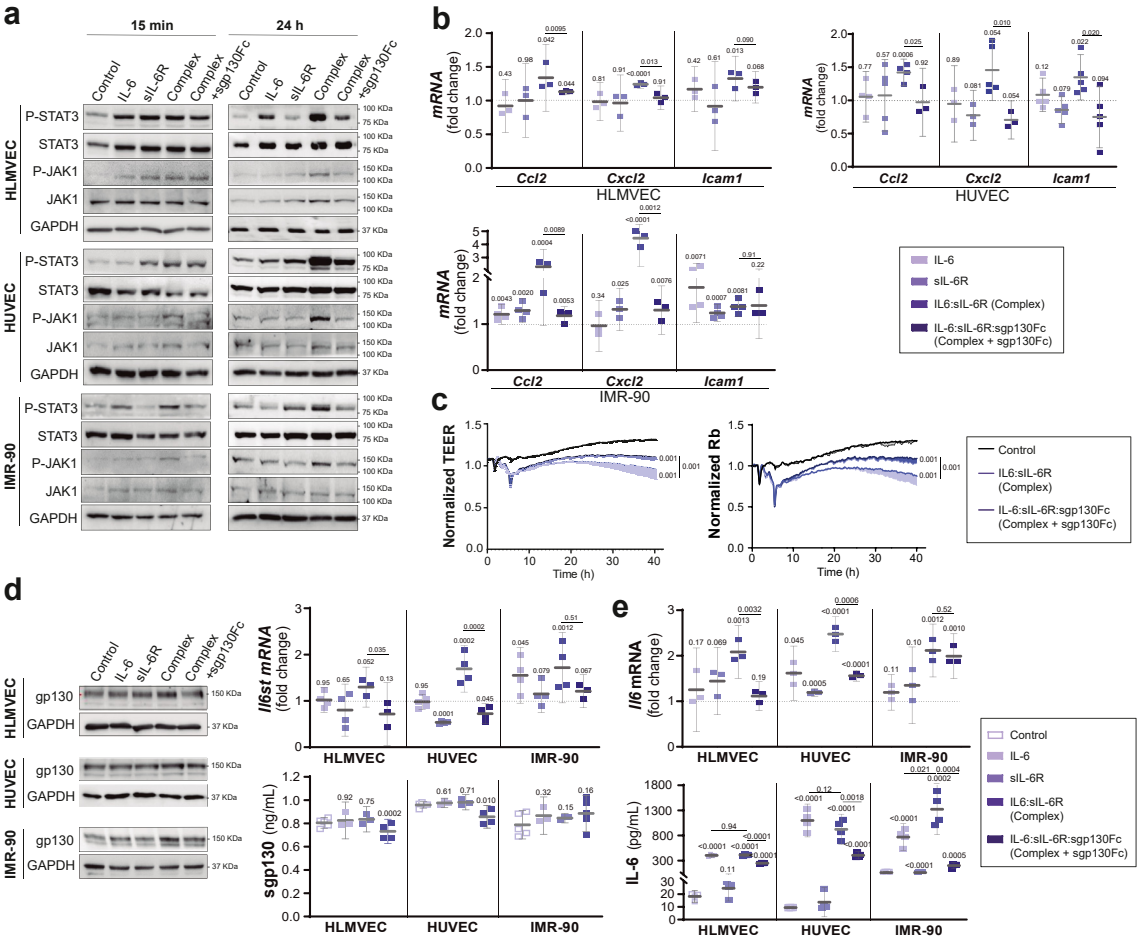

Fig. 7: **Effect of IL-6 trans-signalling on human endothelial cells and lung fibroblasts.** Human lung microvascular endothelial cells (HLMVEC), human umbilical vein endothelial cells (HUVEC) and human lung fibroblast (IMR-90) were treated with vehicle (control), IL-6 (20 ng/mL), IL-6R (20 ng/mL) or IL-6:sIL-6R (Complex, 20 ng/mL) in the presence or absence of sgp130Fc (300 ng/mL). **a)** Representative Western blot of P (Tyr705)-STAT3, STAT3, P (Tr1034/1035)-JAK1 and JAK1 from cell lysates after 15 min and 24 h of treatment. **b)** mRNA expression of proinflammatory markers (*Ccl2*, *Cxcl2* and *Icam1*) by qPCR after 24 h of treatment. **c)** TEER assays performed in HLMVEC stimulated with vehicle (control) and IL-6:sIL-6R complex in the presence or absence of sgp130Fc. TEER was continuously measured for 40 h, and rabbit (Rb) was modelled with the ECIS software. **d)** Representative Western blots, *Il6st* (gp130) mRNA expression by qPCR and gp130 protein levels in supernatants from cultured cells after 24 h of treatment. **e)** *Il6* mRNA expression by qPCR and IL-6 levels by ELISA in supernatants from cultured cells after 24 h of treatment. Data are combined from 4–3 independent experiments. Control is set to 1 for each experiment and data presented as fold-change *vs* control. Complex: IL-6:sIL-6R. Complex + sgp130Fc: IL-6:sIL-6R:sgp130Fc. All graphs show mean and 95% CI. Statistics were calculated by Kruskal Wallis test with Mann–Whitney U-test. *p* values *vs* vehicle-treated control (above) and *vs* complex (bar) are indicated in the graphs.

JAK1 and the downstream STAT3 (Fig. 7a). In this line, the inhibition was in a dose-dependent manner without modifying the viability of the cells (Supplementary Figure S5 and S6). To note, increased mRNA expression of markers of inflammation/adhesion such as *Ccl2* (*Mcp1*), *Cxcl2* and *Icam1* was induced by the IL-6:sIL-6R complex at 24 h and partially blocked by sgp130Fc in all cells (Fig. 7b). Protein levels of ICAM-1 and MCP-1 peaked at 12 h and 24 h respectively and were blocked by sgp130Fc (Supplementary Figure S7). Notably, IL-6:sIL-6R complexes reduced the transendothelial electric resistance (TEER) of a confluent HLMVEC monolayer and sgp130Fc recovered endothelial cell function (Fig. 7c), supporting that vascular leakage described in SARS-CoV-2-infected mice and patients with COVID-19 could be due not only to inflammatory cells, as it has been described,[42] but also as a result of IL-6 trans-signalling.

Since endothelial cells and fibroblasts have scant amount of functional IL-6R,[52] the extent of trans-signalling could depend on the amount of gp130. We observed that gp130 was significantly upregulated at

24 h, both at mRNA and protein level, by IL-6 trans-signalling, although sgp130 in supernatants decreased (Fig. 7d and Supplementary Figure S8). Overexpression of gp130 protein and mRNA was accompanied by increment of *Il6* mRNA expression and IL-6 secretion (Fig. 7e). Altogether, IL-6 trans-signalling could activate an autocrine loop mainly due to the increase of gp130 and IL-6 levels, as it has been reported in vascular smooth muscle cells (VSMC),[53] and recently in endothelial cells.[54]

As a general conclusion of the study, IL-6:sIL-6R complexes induced by SARS-CoV-2-infection are responsible for endothelial cell dysfunction and short and long-term consequences such as oedema, haemorrhage and coagulopathy. Therapeutic intervention with IL-6 trans-signalling blockade by sgp130Fc recovers vascular integrity (Fig. 8).

Discussion

The present study demonstrates that the specific IL-6 trans-signalling blockade by sgp130Fc in a COVID-19 mouse model improves clinical outcomes with a significant reduction of symptomatology and mortality. To note, sgp130Fc treatment improved survival and reduced lung injury in surviving mice. The results show that the specific inhibition of IL-6 trans-signalling constitutes a therapeutic target in acute phase and long-term consequences of SARS-CoV-2 infection. *In vitro*, we demonstrate that human endothelial cells and lung fibroblasts react to cell injury driven by IL-6 trans-signalling through a strong and persisting JAK1/STAT3 activation, partially responding to the inhibition by sgp130Fc. The data point to IL-6 trans-signalling as a main responsible of the pro-inflammatory status, with important implications for the development of COVID-19 therapies.

IL-6 trans-signalling underlies various inflammatory conditions such as autoimmune disease, sepsis, cytokine release syndrome,[55] SARS-CoV-2 infection,[34,37,56] and other chronic conditions: asthma,[57] rheumatoid arthritis,[58] inflammatory bowel disease,[59] neurodegenerative disorders.[60] In COVID-19, it has been reported the role of sIL-6R in the cytokine storm syndrome,[37] and in the procoagulant endotheliopathy mechanisms involved in liver injury.[34] Our group suggested a potential role of IL-6 trans-signalling in patients with severe COVID-19 analysing serum IL-6:sIL-6R and IL-6:sIL-6R:sgp130 complexes.[11] Nevertheless, the importance of IL-6 trans-signalling in SARS-CoV-2 infection consequences has not been fully investigated. Therapies blocking IL-6 receptor such as tocilizumab, sarilumab and the experimental IL-6 antagonist clazakizumab, prevent the binding of IL-6 to IL-6R inhibiting both classic signalling and trans-signalling.[61] Those antibodies reduced inflammatory responses and improved clinical outcomes in patients with COVID-19.[12–15] Since IL-6 classic signalling is considered beneficial and controls viral infection,[62] global inhibition of IL-6 signalling has the potential to increase the risk of infections and viral replication.[63] On the other hand, therapies based on JAK inhibitors, such as baricitinib, have shown good responses in severe COVID-19,[64,65] but are associated with higher frequency of serious infections.[66] Furthermore, JAK pathway is not solely dependent on IL-6

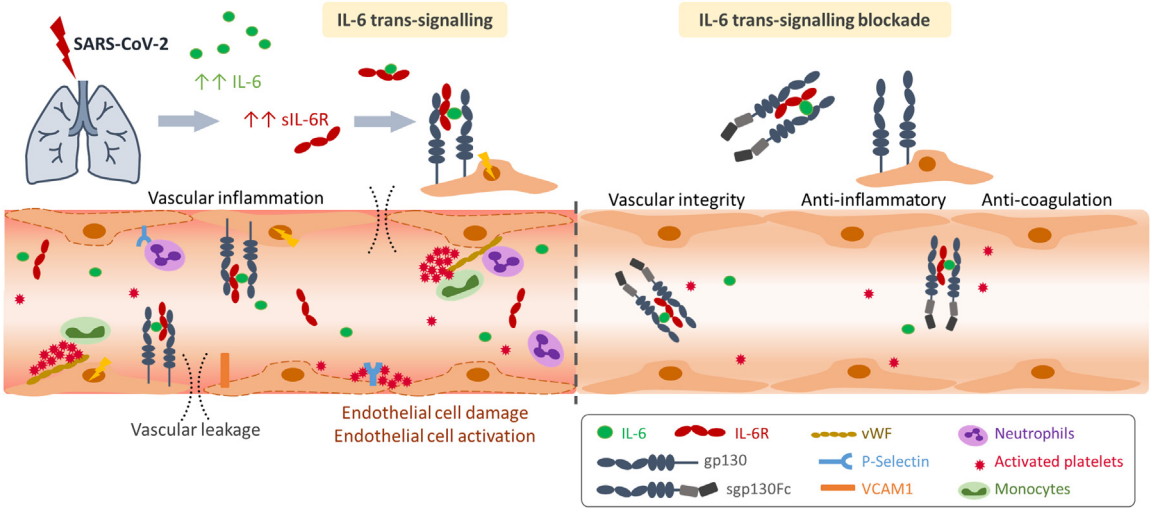

***Fig. 8:* Graphical abstract: IL-6 trans-signalling in SARS-CoV-2 infection on lung microvascular endothelial cells and therapeutic inhibition of IL-6 trans-signalling.** Increased levels of IL-6:sIL-6R complexes observed in SARS-CoV2-infected mice induce endothelial cell dysfunction, widespread endothelial damage, coagulopathy and vascular leakage. Therapeutic IL-6 trans-signalling blockade by sgp130Fc exerts anti-inflammatory and anti-coagulant properties and recovers vascular integrity.

activation, so inhibiting these molecules does not achieve selective blockade of IL-6 signalling. In this context, therapies blocking IL-6:sIL-6R complexes thereby inhibiting only IL-6 trans-signalling,[32] might offer an attractive alternative strategy.

K18-hACE2 transgenic mice infected with SARS-CoV-2 is a valuable model to test potential therapeutic approaches.[27] Here, we show that the specific blockade of IL-6 trans-signalling, using sgp130Fc, reduced symptomatology and mortality in infected mice. Indeed, treated mice exhibited a cumulative symptomatology incidence lower than untreated group and were 66.15% more likely to survive. In this line, sgp130Fc treatment had previously showed increase of survival rate in a mouse model of sepsis with 100% and 80% of survival associated to preventive and therapeutic treatment, respectively.[30] In our experimental design, the treatment was administered in two doses after virus inoculation (at two and eight dpi). Since viral load was similar between treated and untreated groups, we postulate that increased survival rates and improvement of health-associated parameters (symptomatology and lung injury) were due to the sgp130Fc treatment. The results point out the importance of IL-6 trans-signalling in the pathogenesis of severe COVID-19,[11,37] and suggest that this signalling mode can be selectively targeted to improve the course of the disease.

SARS-CoV-2 infection in K18-hACE2 mice elicited a quantifiable level of systemic pro-inflammatory cytokines and cell-recruiting chemokines (IL-6, CXCL10, CCL5 and CCL11) which were linked to mortality. Importantly, we observed a significant decrease of sIL-6R levels in untreated dead/euthanized mice (<15 dpi) compared to survivors (15 dpi). These results are in line with our previous report in human patients with COVID-19, in which the combination of increased IL-6 and reduced sIL-6R serum levels was an accurate predictor of death in the context of lymphopenia, probably reflecting a profound dysregulation of the protective immunity that contributes to the fatal outcome.[11] However, in surviving mice (15 dpi), sgp130Fc treatment significantly decreased serum IL-6 and sIL-6R levels along with lung mRNA expression of *Tnfα*, *Il1ß*, *Ifnγ* and other cytokines belonging to IL-6 family related with severity of COVID-19 such as *Osm*, *Lif* and *Il11*.[40,41,67] Regarding sIL-6R, our group and others have reported significant increased serum levels in survivor patients with severe COVID-19,[11,68] likely due to the release from activated T cells.[69] In this context, sgp130Fc treatment showed a clear anti-inflammatory effect with potential impact in long term consequences of the disease. Consequently, the histopathological analyses revealed marked differences between untreated and treated surviving animals (15 dpi), that exhibited a significant reduction of the inflammatory infiltrate. Untreated mice presented increased number of inflammatory foci with lymphocytes and macrophages expanding in the interalveolar spaces with cumulative deposition of collagen, and thickened collagen bundles in the lung parenchyma, as it has been described in the humanized MISTRG6-hACE2 mice model of chronic COVID-19 at 14 dpi.[70] These findings have been related with the grave and persistent lung pathology observed in patients with severe COVID-19.[36,70] Therefore, the data indicate that sgp130Fc may be an interesting prognostic and therapeutic tool for acute phase and long-term consequences of COVID-19. Although, our experimental setting could be considered restricted (15 dpi), which might be a possible limitation of the study, we detected important differences in the histological and immunohistochemical analysis, and pro-inflammatory markers profile, between treated and untreated groups, with marked improvement of lung injury in sgp130Fc-treated mice. Furthermore, in a previously reported 28 dpi-established chronic model of COVID-19, characteristic histopathological changes in the lung, similar to the ones observed in our study, were detected as soon as 14 dpi.[70] In this sense, our data at 15 dpi suggest the potential benefits of sgp130Fc treatment in the long-term consequences of SARS-CoV-2 infection. Nevertheless, more studies focusing on the effects of sgp130Fc in long-term consequences of COVID-19 would be desirable.

SARS-CoV-2-infected surviving mice (15 dpi) developed endothelial dysfunction in lung vessels suggested by upregulation of endothelial cell activation markers and loss of the vascular barrier integrity. In this context, it has been suggested that the damage across diverse tissues observed in COVID-19 is not only due to the direct effect of the virus, but mainly to the inflammation and the immune-mediated response.[71] SARS-CoV-2 spike protein promotes IL-6 trans-signalling, being responsible for the endothelial cell damage, capillary inflammation and thrombosis.[34,56] Surviving sgp130Fc-treated mice (15 dpi) showed significant decrease of lung damage, inflammation and procoagulant endotheliopathy (vWF expression and platelet accumulation) compared to untreated animals. Our data suggest that IL-6 trans-signalling is the mechanistic link between endothelial cells activation and COVID-19 in lung damage, as it has been described in the liver,[34] and that the specific inhibition of this IL-6 signalling mode ameliorates lung injury in surviving mice. It is important to note that patients with severe SARS-CoV-2 infection present a prothrombotic state leading to thromboembolic complications.[47] Therefore, IL-6 trans-signalling inhibition could offer a potential therapy for those patients. Our data also showed that sgp130Fc treatment is responsible for the inhibitory effect on the STAT3 target genes in lungs from surviving treated mice. Altogether, we demonstrate the *in vivo* efficacy of IL-6 trans-signalling blockade and the association of reduced expression of STAT3 pathway genes with improved rates of mortality and morbidity. At the same time, our data reveal the potential therapeutic role of

sgp130Fc not only in the progression of COVID-19 in the first days, but also to prevent the lung damage observed in the post-acute phase of the disease.

We recognize certain limitations and con-founding factors in this study: i) We examined the performance of IL-6 trans-signalling blockade with a single dose of sgp130Fc; which has been reported to inhibit only trans-signalling. Nevertheless, we demonstrate that at the dose of 1 mg/kg sgp130Fc reduced severity and mortality and reduced the expression of *Stat3* and target genes in lung samples; thus, it could be suggested that the dose was sufficient to inhibit IL-6 trans-signalling in surviving treated mice. ii) We did not consider the effect of sgp130Fc in the blockade of IL-11 trans-signalling as a confounding factor that may have an impact in the therapeutic effect. However, the effect of IL-11 in COVID-19 is unknown, we did not see a clear increase of this cytokine in SARS-CoV-2 infected mice, and it may be expected that the activity of IL-11 is more closely linked to the parenchymal biology.[72] iii) Although SARS-CoV-2-infected K18-hACE2 mice closely display the phenotypes observed in patient with severe COVID-19,[22] and it has been used to evaluate experimental interventions,[27] species specific immune response to the infection may constitute a confounding factor. iv) We acknowledge possible bias in HR, but our follow-up was sufficient to obtain relevant clinical information about the effect of the treatment. Moreover, the survival curve offered information about the distribution of the events. v) Age, sex, variances in the animal microbiome, virus strain, mutations and titter, could differentially affect the outcomes.

IL-6 trans-signalling induced strong and persisting downstream signalling in primary endothelial cells and lung fibroblasts, with increase expression of chemokines and adhesion molecules that could promote inflammatory cell recruitment. Importantly, the presence of IL-6:sIL-6R complex upregulated the expression of gp130 and induced IL-6 secretion. It has been assumed that those factors could maintain IL-6 trans-signalling in cells with scant amount of IL-6R as VSMC,[53] and endothelial cells,[54] in which this receptor is not expressed.[52] To note, immune cells are the main source of IL-6R,[73] providing the third component necessary for IL-6 signalling. In this context, our data show that IL-6:sIL-6R complex induces the expression of chemokines, mainly *Ccl2* and *Cxcl2* as well as the adhesion molecule *Icam1* in endothelial cells and lung fibroblasts. Thus, IL-6 trans-signalling in those cells, through the increase of gp130 and IL-6 together with IL-6R from immune cells, could activate an autocrine loop amplifying its proinflammatory role. Importantly, the presence of sgp130Fc partially reduced the expression of chemokines, IL-6 and gp130. Altogether, our results show a link between IL-6 trans-signalling and the amplification of the proinflammatory status and endotheliopathy.

In conclusion, we demonstrate that the specific blockade of IL-6 trans-signalling has a great potential to mitigate both, acute phase and long-term consequences of SARS-CoV-2 infection. The study provides important information to understand the pathogenesis of the disease. Overall, these results place IL-6 trans-signalling as a main driver of pro-inflammatory events underlying COVID-19, and point to therapies focused on the specific inhibition of this mode of IL-6 signalling as promising tools in the prognosis and treatment of the disease.

Contributors

MAR-H, SR-J, CVK and MB conceptualized and designed the study. MAR-H, CS, MB-B, DC and CZ-P conducted the investigations. MAR-H, SR-J, CVK, CS, MB, JM, PMP and FJP, conducted formal data analysis. MAR-H, SR-J and MB wrote the original first draft of manuscript. All authors reviewed the manuscript and gave significant input. MAR-H and MB had access to and verified all underlying data. The final version of this paper was reviewed and approved by all authors.

Data sharing statement

All relevant data have been presented in the manuscript. All requests for or questions about the data can be initiated by contacting marodriguez-ibis@us.es and mbustos-ibis@us.es.

Declaration of interests

SR-J has acted as a consultant and speaker for AbbVie, Chugai, Genentech Roche, Regeneron, Pfizer, and Sanofi. He also declares that he is an inventor on patents owned by CONARIS Research Institute, which develops the sgp130Fc protein olamkicept together with Ferring Pharmaceuticals and I-Mab Biopharma. SR-J has stock ownership in CONARIS. DC is supported by iPFIS, ISCIII (IFI 19/00048). CZP held a contract from the Programa de Garantía Juvenil. All other authors have no conflicts of interest to disclose.

Acknowledgements

This study has been funded by Instituto de Salud Carlos III (ISCIII) through the projects PI23/01351 (to MARH) and COV-20/00792 (to MB), and co-funded by the European Union; and by the European Commission—Next generation EU (European Union) (Regulation EU 2020/2094), through CSIC's Global Health Platform (PTI Salud Global,) (SGL2103029 to MB). PID2019-110587RB-I00 (MB) supported by MICIN/AEI/10.13039/501100011033/and PID2022-143034OB-I00 (MB) by MICIN/AEI/10.13039/501100011033/FEDER. MAR-H acknowledges support from ISCIII, Spain and the European Commission—Next generation EU (European Union), through CSIC's Global Health PTI. The authors thank to the Gabinete Veterinario (UAM); Centro de Vigilancia Sanitaria Veterinaria (VISAVET); IBiS histopathology facility; IBiS microscopy service; Statistics and Research Methodology Unit of the Andalusian Public Foundation for Health Research Management of Seville (FISEVI) (special thanks to Henry A. Andrade Ruiz for the statistical advice on this study); Cristina Olagüe and Gloria González-Aseguinolaza (CIMA) for providing virus.

Appendix A. Supplementary data

Supplementary data related to this article can be found at https://doi.org/10.1016/j.ebiom.2024.105132.

References

1 Mongin D, Burgisser N, Laurie G, et al. Effect of SARS-CoV-2 prior infection and mRNA vaccination on contagiousness and susceptibility to infection. *Nat Commun*. 2023;14(1):5452.
2 Goshua G, Pine AB, Meizlish ML, et al. Endotheliopathy in COVID-19-associated coagulopathy: evidence from a single-centre, cross-sectional study. *Lancet Haematol*. 2020;7(8):e575–e582.

3 Yuki K, Fujiogi M, Koutsogiannaki S. COVID-19 pathophysiology: a review. *Clin Immunol*. 2020;215:108427.
4 D'Agnillo F, Walters KA, Xiao Y, et al. Lung epithelial and endothelial damage, loss of tissue repair, inhibition of fibrinolysis, and cellular senescence in fatal COVID-19. *Sci Transl Med*. 2021;13(620):eabj7790.
5 Xu SW, Ilyas I, Weng JP. Endothelial dysfunction in COVID-19: an overview of evidence, biomarkers, mechanisms and potential therapies. *Acta Pharmacol Sin*. 2023;44(4):695–709.
6 Noris M, Benigni A, Remuzzi G. The case of complement activation in COVID-19 multiorgan impact. *Kidney Int*. 2020;98(2):314–322.
7 Felsenstein S, Herbert JA, McNamara PS, Hedrich CM. COVID-19: immunology and treatment options. *Clin Immunol*. 2020;215:108448.
8 Giraldez MD, Carneros D, Garbers C, Rose-John S, Bustos M. New insights into IL-6 family cytokines in metabolism, hepatology and gastroenterology. *Nat Rev Gastroenterol Hepatol*. 2021;18(11):787–803.
9 Veras FP, Pontelli MC, Silva CM, et al. SARS-CoV-2-triggered neutrophil extracellular traps mediate COVID-19 pathology. *J Exp Med*. 2020;217(12):e20201129.
10 Middleton EA, He XY, Denorme F, et al. Neutrophil extracellular traps contribute to immunothrombosis in COVID-19 acute respiratory distress syndrome. *Blood*. 2020;136(10):1169–1179.
11 Rodríguez-Hernández MÁ, Carneros D, Núñez-Núñez M, et al. Identification of IL-6 signalling components as predictors of severity and outcome in COVID-19. *Front Immunol*. 2022;13:891456.
12 Ghosn L, Chaimani A, Evrenoglou T, et al. Interleukin-6 blocking agents for treating COVID-19: a living systematic review. *Cochrane Database Syst Rev*. 2021;3(3):CD013881.
13 Chen JJ, Zhang LN, Hou H, Xu L, Ji K. Interleukin-6 signaling blockade treatment for cytokine release syndrome in COVID-19 (Review). *Exp Ther Med*. 2021;21(1):24.
14 Abidi E, El Nekidy WS, Alefishat E, et al. Tocilizumab and COVID-19: timing of administration and efficacy. *Front Pharmacol*. 2022;13:825749.
15 Albuquerque AM, Eckert I, Tramujas L, et al. Effect of tocilizumab, sarilumab, and baricitinib on mortality among patients hospitalized for COVID-19 treated with corticosteroids: a systematic review and meta-analysis. *Clin Microbiol Infect*. 2023;29(1):13–21.
16 Lang VR, Englbrecht M, Rech J, et al. Risk of infections in rheumatoid arthritis patients treated with tocilizumab. *Rheumatology (Oxford)*. 2012;51(5):852–857.
17 Peng J, Fu M, Mei H, et al. Efficacy and secondary infection risk of tocilizumab, sarilumab and anakinra in COVID-19 patients: a systematic review and meta-analysis. *Rev Med Virol*. 2022;32(3):e2295.
18 Rose-John S, Jenkins BJ, Garbers C, Moll JM, Scheller J. Targeting IL-6 trans-signalling: past, present and future prospects. *Nat Rev Immunol*. 2023;23(10):666–681.
19 Schreiber S, Aden K, Bernardes JP, et al. Therapeutic interleukin-6 trans-signaling inhibition by olamkicept (sgp130Fc) in patients with active inflammatory bowel disease. *Gastroenterology*. 2021;160(7):2354–2366.e11.
20 Zhang S, Chen B, Wang B, et al. Effect of induction therapy with olamkicept vs placebo on clinical response in patients with active ulcerative colitis: a randomized clinical trial. *JAMA*. 2023;329(9):725–734.
21 Ettich J, Werner J, Weitz HT, et al. A hybrid soluble gp130/spike-nanobody fusion protein simultaneously blocks interleukin-6 trans-signaling and cellular infection with SARS-CoV-2. *J Virol*. 2022;96(4):e0162221.
22 Winkler MS, Skirecki T, Brunkhorst FM, et al. Bridging animal and clinical research during SARS-CoV-2 pandemic: a new-old challenge. *eBioMedicine*. 2021;66:103291.
23 Dong W, Mead H, Tian L, et al. The K18-human ACE2 transgenic mouse model recapitulates non-severe and severe COVID-19 in response to an infectious dose of the SARS-CoV-2 virus. *J Virol*. 2022;96(1):e0096421.
24 Oladunni FS, Park JG, Pino PA, et al. Lethality of SARS-CoV-2 infection in K18 human angiotensin-converting enzyme 2 transgenic mice. *Nat Commun*. 2020;11(1):6122.
25 Radvak P, Kwon HJ, Kosikova M, et al. SARS-CoV-2 B.1.1.7 (alpha) and B.1.351 (beta) variants induce pathogenic patterns in K18-hACE2 transgenic mice distinct from early strains. *Nat Commun*. 2021;12(1):6559.
26 Stolp B, Stern M, Ambiel I, et al. SARS-CoV-2 variants of concern display enhanced intrinsic pathogenic properties and expanded organ tropism in mouse models. *Cell Rep*. 2022;38(7):110387.
27 Pastor-Fernandez A, Bertos AR, Sierra-Ramirez A, et al. Treatment with the senolytics dasatinib/quercetin reduces SARS-CoV-2-related mortality in mice. *Aging Cell*. 2023;22(3):e13771.
28 Jiang RD, Liu MQ, Chen Y, et al. Pathogenesis of SARS-CoV-2 in transgenic mice expressing human angiotensin-converting enzyme 2. *Cell*. 2020;182(1):50–58.e8.
29 Twitchell DK, Christensen MB, Hackett G, Morgentaler A, Saad F, Pastuszak AW. Examining male predominance of severe COVID-19 outcomes: a systematic review. *Androg Clin Res Ther*. 2022;3(1):41–53.
30 Barkhausen T, Tschernig T, Rosenstiel P, et al. Selective blockade of interleukin-6 trans-signaling improves survival in a murine polymicrobial sepsis model. *Crit Care Med*. 2011;39(6):1407–1413.
31 Aparicio B, Casares N, Egea J, et al. Preclinical evaluation of a synthetic peptide vaccine against SARS-CoV-2 inducing multi-epitopic and cross-reactive humoral neutralizing and cellular CD4 and CD8 responses. *Emerg Microbes Infect*. 2021;10(1):1931–1946.
32 Jostock T, Mullberg J, Ozbek S, et al. Soluble gp130 is the natural inhibitor of soluble interleukin-6 receptor transsignaling responses. *Eur J Biochem*. 2001;268(1):160–167.
33 Granai M, Warm V, Vogelsberg A, et al. Impact of P-selectin-PSGL-1 Axis on platelet-endothelium-leukocyte interactions in fatal COVID-19. *Lab Invest*. 2023;103(8):100179.
34 McConnell MJ, Kawaguchi N, Kondo R, et al. Liver injury in COVID-19 and IL-6 trans-signaling-induced endotheliopathy. *J Hepatol*. 2021;75(3):647–658.
35 Colas-Algora N, Munoz-Pinillos P, Cacho-Navas C, et al. Simultaneous targeting of IL-1-signaling and IL-6-trans-signaling preserves human pulmonary endothelial barrier function during a cytokine storm-brief report. *Arterioscler Thromb Vasc Biol*. 2023;43(11):2213–2222.
36 Rendeiro AF, Ravichandran H, Bram Y, et al. The spatial landscape of lung pathology during COVID-19 progression. *Nature*. 2021;593(7860):564–569.
37 Chen LYC, Biggs CM, Jamal S, Stukas S, Wellington CL, Sekhon MS. Soluble interleukin-6 receptor in the COVID-19 cytokine storm syndrome. *Cell Rep Med*. 2021;2(5):100269.
38 Gebremeskel S, Schanin J, Coyle KM, et al. Mast cell and eosinophil activation are associated with COVID-19 and TLR-mediated viral inflammation: implications for an anti-siglec-8 antibody. *Front Immunol*. 2021;12:650331.
39 Villeda SA, Luo J, Mosher KI, et al. The ageing systemic milieu negatively regulates neurogenesis and cognitive function. *Nature*. 2011;477(7362):90–94.
40 Arunachalam PS, Wimmers F, Mok CKP, et al. Systems biological assessment of immunity to mild versus severe COVID-19 infection in humans. *Science*. 2020;369(6508):1210–1220.
41 Ciceri P, Bono V, Magagnoli L, et al. Cytokine and chemokine retention profile in COVID-19 patients with chronic kidney disease. *Toxins (Basel)*. 2022;14(10):673.
42 Allnoch L, Beythien G, Leitzen E, et al. Vascular inflammation is associated with loss of aquaporin 1 expression on endothelial cells and increased fluid leakage in SARS-CoV-2 infected golden Syrian hamsters. *Viruses*. 2021;13(4):639.
43 Goncalves-Pereira MH, Santiago L, Ravetti CG, et al. Dysfunctional phenotype of systemic and pulmonary regulatory T cells associate with lethal COVID-19 cases. *Immunology*. 2023;168(4):684–696.
44 Zheng J, Wong LR, Li K, et al. COVID-19 treatments and pathogenesis including anosmia in K18-hACE2 mice. *Nature*. 2021;589(7843):603–607.
45 Winkler ES, Bailey AL, Kafai NM, et al. SARS-CoV-2 infection of human ACE2-transgenic mice causes severe lung inflammation and impaired function. *Nat Immunol*. 2020;21(11):1327–1335.
46 Pober JS. Activation and injury of endothelial cells by cytokines. *Pathol Biol (Paris)*. 1998;46(3):159–163.
47 Barbosa LC, Goncalves TL, de Araujo LP, Rosario LVO, Ferrer VP. Endothelial cells and SARS-CoV-2: an intimate relationship. *Vascul Pharmacol*. 2021;137:106829.
48 de Rooij L, Becker LM, Carmeliet P. A role for the vascular endothelium in post-acute COVID-19? *Circulation*. 2022;145(20):1503–1505.
49 Babkina AS, Ostrova IV, Yadgarov MY, et al. The role of von Willebrand factor in the pathogenesis of pulmonary vascular thrombosis in COVID-19. *Viruses*. 2022;14(2):211.

50 Won T, Wood MK, Hughes DM, et al. Endothelial thrombomodulin downregulation caused by hypoxia contributes to severe infiltration and coagulopathy in COVID-19 patient lungs. *eBioMedicine*. 2022;75:103812.
51 Ashour L. Roles of the ACE/Ang II/AT1R pathway, cytokine release, and alteration of tight junctions in COVID-19 pathogenesis. *Tissue Barriers*. 2023;11(2):2090792.
52 Romano M, Sironi M, Toniatti C, et al. Role of IL-6 and its soluble receptor in induction of chemokines and leukocyte recruitment. *Immunity*. 1997;6(3):315–325.
53 Klouche M, Bhakdi S, Hemmes M, Rose-John S. Novel path to activation of vascular smooth muscle cells: up-regulation of gp130 creates an autocrine activation loop by IL-6 and its soluble receptor. *J Immunol*. 1999;163(8):4583–4589.
54 Gatsiou A, Tual-Chalot S, Napoli M, et al. The RNA editor ADAR2 promotes immune cell trafficking by enhancing endothelial responses to interleukin-6 during sterile inflammation. *Immunity*. 2023;56(5):979–997.e11.
55 Tanaka T, Narazaki M, Kishimoto T. Immunotherapeutic implications of IL-6 blockade for cytokine storm. *Immunotherapy*. 2016;8(8):959–970.
56 Patra T, Meyer K, Geerling L, et al. SARS-CoV-2 spike protein promotes IL-6 trans-signaling by activation of angiotensin II receptor signaling in epithelial cells. *PLoS Pathog*. 2020;16(12):e1009128.
57 Jevnikar Z, Ostling J, Ax E, et al. Epithelial IL-6 trans-signaling defines a new asthma phenotype with increased airway inflammation. *J Allergy Clin Immunol*. 2019;143(2):577–590.
58 Cronstein BN. Interleukin-6–a key mediator of systemic and local symptoms in rheumatoid arthritis. *Bull NYU Hosp Jt Dis*. 2007;65(Suppl 1):S11–S15.
59 Chalaris A, Schmidt-Arras D, Yamamoto K, Rose-John S. Interleukin-6 trans-signaling and colonic cancer associated with inflammatory bowel disease. *Dig Dis*. 2012;30(5):492–499.
60 Campbell IL, Erta M, Lim SL, et al. Trans-signaling is a dominant mechanism for the pathogenic actions of interleukin-6 in the brain. *J Neurosci*. 2014;34(7):2503–2513.
61 Kang S, Tanaka T, Narazaki M, Kishimoto T. Targeting interleukin-6 signaling in clinic. *Immunity*. 2019;50(4):1007–1023.
62 Kopf M, Baumann H, Freer G, et al. Impaired immune and acute-phase responses in interleukin-6-deficient mice. *Nature*. 1994;368(6469):339–342.
63 Pawar A, Desai RJ, Solomon DH, et al. Risk of serious infections in tocilizumab versus other biologic drugs in patients with rheumatoid arthritis: a multidatabase cohort study. *Ann Rheum Dis*. 2019;78(4):456–464.
64 Kalil AC, Stebbing J. Baricitinib: the first immunomodulatory treatment to reduce COVID-19 mortality in a placebo-controlled trial. *Lancet Respir Med*. 2021;9(12):1349–1351.
65 Marconi VC, Ramanan AV, de Bono S, et al. Efficacy and safety of baricitinib for the treatment of hospitalised adults with COVID-19 (COV-BARRIER): a randomised, double-blind, parallel-group, placebo-controlled phase 3 trial. *Lancet Respir Med*. 2021;9(12):1407–1418.
66 Praveen D, Puvvada RC, M VA. Janus kinase inhibitor baricitinib is not an ideal option for management of COVID-19. *Int J Antimicrob Agents*. 2020;55(5):105967.
67 Lopez-Ayllon BD, de Lucas-Rius A, Mendoza-Garcia L, et al. SARS-CoV-2 accessory proteins involvement in inflammatory and profibrotic processes through IL11 signaling. *Front Immunol*. 2023;14:1220306.
68 Koutsakos M, Rowntree LC, Hensen L, et al. Integrated immune dynamics define correlates of COVID-19 severity and antibody responses. *Cell Rep Med*. 2021;2(3):100208.
69 Briso EM, Dienz O, Rincon M. Cutting edge: soluble IL-6R is produced by IL-6R ectodomain shedding in activated CD4 T cells. *J Immunol*. 2008;180(11):7102–7106.
70 Sefik E, Israelow B, Mirza H, et al. A humanized mouse model of chronic COVID-19. *Nat Biotechnol*. 2022;40(6):906–920.
71 Davis HE, McCorkell L, Vogel JM, Topol EJ. Long COVID: major findings, mechanisms and recommendations. *Nat Rev Microbiol*. 2023;21(3):133–146.
72 Wang D, Zheng X, Fu B, et al. Hepatectomy promotes recurrence of liver cancer by enhancing IL-11-STAT3 signaling. *eBioMedicine*. 2019;46:119–132.
73 Kang S, Kishimoto T. Interplay between interleukin-6 signaling and the vascular endothelium in cytokine storms. *Exp Mol Med*. 2021;53(7):1116–1123.